Received: 10 April 2025 | Accepted: 18 April 2025

DOI: 10.1002/ecs2.70324

ECOSPHERE
AN ESA OPEN ACCESS JOURNAL

ARTICLE
Disease Ecology

Parasite spatial distribution shapes parasite aggregation on host populations, but not at high parasite density

Chris Wojan | **Allison K. Shaw** | **Meggan E. Craft**

Department of Ecology, Evolution, and Behavior, University of Minnesota, St. Paul, Minnesota, USA

Correspondence
Chris Wojan
Email: cwojan@gmail.com

Funding information
Division of Environmental Biology, Grant/Award Number: DEB-2321358

Handling Editor: Sunshine A. Van Bael

Abstract

Spatial aggregation of environmental or trophically transmitted parasites has the potential to influence host–parasite interactions. The distribution of parasites on hosts is one result of those interactions, and the role of spatial aggregation is unclear. We use a spatially explicit agent-based model to determine how spatial aggregation of parasites influences the distribution of parasite burdens across a range of parasite densities and host recovery rates. Our model simulates the random movement of hosts across landscapes with varying spatial configurations of areas occupied by environmental parasites, allowing hosts to acquire parasites they encounter and subsequently lose them. When parasites are more spatially aggregated in the environment, the aggregation of parasite burdens on hosts is higher (i.e., more hosts with few parasites, fewer hosts with many parasites), but the effect is less pronounced at high parasite density and fast host recovery rates. In addition, the correlation between individual hosts' final parasite burdens and their cumulative parasite burdens (including lost parasites) is greater at higher levels of spatial parasite aggregation. Our work suggests that fine-scale spatial patterns of parasites can play a strong role in shaping how hosts are parasitized, particularly when parasite density is low-to-moderate and recovery rates are slow.

KEYWORDS
agent-based model, parasite aggregation, parasite ecology, spatial distribution

INTRODUCTION

Spatial patterns of parasites and hosts influence their interactions with each other (Albery et al., 2019; Bonnell et al., 2018; Mollison & Levin, 1995; Nunn et al., 2011). In particular, the spatial distribution of macroparasites, or parasites visible to the naked eye, relative to the hosts they parasitize can explain heterogeneous infection among those hosts (Keymer & Anderson, 1979; Lutermann et al., 2012; Wilson et al., 2002). In a given habitat, macroparasites may spatially vary in abundance due to chance or microclimate suitability. This spatial heterogeneity is most likely to affect host population parasitism patterns in the case of multi-host environmental and trophically transmitted parasites, as their spatial distribution is driven by processes not directly related to the host in question (e.g., deposition by other host species, location of infected prey). For example, gravid adult deer ticks (*Ixodes scapularis*) are deposited into the environment by white-tailed deer (Dumas et al., 2022), and subsequent

juvenile tick abundance is correlated with vegetation, temperature, and relative humidity (Ginsberg et al., 2020; Mathisson et al., 2021), and thus, the spatial distribution of juvenile ticks is independent of the small mammal hosts they go on to parasitize. In addition, freshwater fish encounter the parasitic copepod *Tracheliastes polycolpus* predominantly in fine-scale microhabitats with similar stream velocity and substrate size combinations (Mathieu-Bégné et al., 2022). Yet, the finer-scale spatial patterns of parasitism and their ecological consequences are relatively understudied (Albery et al., 2022).

One potential consequence of macroparasite spatial heterogeneity is the aggregation of parasites on hosts, that is, the degree to which a host population consists of few hosts with many parasites and many hosts with few or no parasites (Shaw et al., 1998; Shaw & Dobson, 1995). Parasite aggregation on hosts can in turn have further ecological consequences, like in disease transmission where the few heavily infected individuals can be potential super-spreaders (Rabajante, 2023). Specifically for tick-borne disease, the basic reproductive number of pathogens (the number of new infections expected from an infectious individual during its infectious period in an uninfected population) increases with greater aggregation of ticks on small mammal hosts (Harrison & Bennett, 2012). Additionally, macroparasite aggregation can be used to estimate host mortality in wildlife populations (Wilber et al., 2020).

The causes of parasite aggregation are numerous and have been investigated both experimentally and observationally. Keymer and Anderson (1979) found that more spatially aggregated arrangements of environmental parasites led to greater aggregation of host–parasite burdens in *Tribolium confusum*. However, parasite density in the experiment was held constant, and the work has not been replicated in other systems; thus, the general conditions most suitable for this pattern to emerge remain unclear. Observational studies have shown that individual host characteristics can influence macroparasite burdens. For example, male white-footed mice harbored more larval ticks irrespective of tick spatial aggregation, and larger males with larger home ranges harbored more nymphal ticks (Devevey & Brisson, 2012). Additionally, more exploratory Siberian chipmunks had higher tick loads (Boyer et al., 2010), and reduced immune response was associated with higher endoparasite burdens in both Pacific chorus frogs (Johnson & Hoverman, 2014) and rainbow trout (Tinsley et al., 2020). However, other observational research finds no role of individual host attributes in determining burdens, which by the process of elimination suggests a larger role of spatial aggregation of parasites in the environment (Lutermann et al., 2012). In addition, one study shows that local tick density is the primary driver of individual tick burdens in *Peromyscus leucopus* (Calabrese et al., 2011). Given these contradictory results, it is likely that burden distributions are shaped by a combination of host characteristics and parasite spatial patterns, with the effect of each dependent on the context.

Due to the limitations of past experimental and observational work, theoretical modeling is an ideal tool to better understand the link between parasite spatial aggregation and the aggregation of parasites on host populations. Experimental research to date has not examined the robustness and generality of the relationship, and observational studies cannot feasibly sample the spatial distribution of parasites and their hosts' burdens in the same place simultaneously, as sampling the parasites themselves would either interfere with how the hosts will encounter them in the future, or not be representative of how the hosts encountered them previously. Additionally, individual host differences can play a role in shaping their parasite burdens in both approaches. A simulation model can bypass these problems by explicitly observing the acquisition of parasites by hosts across a wide parameter space of purposefully manipulated parasite spatial arrangements (varying in both spatial aggregation and density), independent of individual variance of host characteristics. Here, we use an agent-based model to explore the interaction between the spatial aggregation of parasites and the density of those parasites on the landscape in driving parasite aggregation on host populations. We predict that more spatially aggregated parasite distributions will lead to more aggregated host–parasite burdens when parasite density is lower. This is because the variation in parasite encounter rate among hosts by location will be higher compared to when parasites saturate the landscape, and every host is frequently encountering parasites. We further expect that this pattern may be sensitive to changes in the rates at which hosts acquire and lose parasites. When recovery from parasites (or loss of parasites) is slower, hosts will have a greater chance of accumulating high burdens. Thus, we predict the most aggregated host–parasite burdens will be observed when parasite loss/recovery is slow and spatial parasite aggregation is high. This is because many hosts will encounter few parasites (due to spatial aggregation), and the few hosts that encounter many parasites will keep them longer, allowing for higher maximum burdens.

MATERIALS AND METHODS

To achieve our research objective, we developed a spatially explicit agent-based model. We describe this model using the Overview, Design Concepts, Details framework

that was introduced in Grimm et al. (2006) and subsequently updated (Grimm et al., 2010, 2020). Our model was developed and run using R version 4.4.1 (R Core Team, 2024) with the following packages: tidyverse version 2.0.0 (Wickham et al., 2019), som.nn version 1.4.4 (Dominik, 2024), ape version 5.8 (Paradis & Schliep, 2019), future version 1.33.2 (Bengtsson, 2021), and furrr version 0.3.1 (Vaughan & Dancho, 2022). For comparison, we also developed a non-spatial model in R based on compound probability distributions (see Appendix S1). The code is available here: https://doi.org/10.5281/zenodo.15360216.

Purpose

The model's purpose is to understand the role of parasite density and spatial aggregation in shaping the distribution of parasite burdens among individual hosts in a population.

Entities, state variables, and scales

The model is composed of three entities—landscape cells, individual hosts, and parasites (Table 1). The state variables of landscape cells are their location and whether they can transmit parasites to hosts (i.e., it is occupied by an environmentally or trophically transmitted parasite). Because the model is not specific to any given system, the landscape cells are of identical, arbitrary size, and arranged in a 48 × 48 torus. The arrangement of landscape cells varies among simulations in (1) the proportion of parasite-occupied cells (our representation of parasite density); and (2) the spatial aggregation of those cells on the torus. The state variables of the individual hosts are their location (landscape cell), the number of parasites they have ever acquired, and the number of parasites they currently have (parasite burden). The state variables of parasites are the host they are parasitizing and the duration of their infection. Individual hosts occupy the landscape cells that match their location, while parasites are simply linked to their hosts.

TABLE 1 List of model entities, parameters, and variables.

Parameter/variable	Variability among simulations	Variability within simulations
Landscape cells		
Landscape size	Constant: 48 × 48 cells	Constant
Proportion of landscape parasite-occupied	0.1–0.9	Constant
Spatial autocorrelation of parasite-occupied landscape cells (Moran's *I*)	~0 to ~0.2	Constant value and spatial configuration
Individual hosts		
Initial location	Random landscape cell	N/A
Probability of parasite acquisition on parasite-occupied cells	Constant: 0.5	Constant
Recovery rate from parasites	0.05, 0.15, 0.25	Constant
Environmental parasites		
Infection duration	Based on host recovery rate	Each parasite's duration from negative binomial distribution, success probability = recovery rate

Abbreviation: N/A, not applicable.

Process overview and scheduling

The model runs through a series of timesteps that represent the time period in which the host-relevant parasite life stage is active (e.g., peak larval tick activity for small mammals). During each timestep, each individual host either stays in its landscape cell or moves to an adjacent one. Then, if the cell a host is occupying is parasite-occupied, the host has some probability of acquiring a new parasite, adding to its parasite burden. Any newly acquired parasite is given a probabilistic infection duration, or number of timesteps until it is no longer parasitizing the host. Parasites exist in the model only for as long as they are linked to a specific host—as this model represents multi-host environmental or trophically transmitted parasites, we assume that after parasites are lost from hosts they move on to their next life stage or reproduce and die. Finally, any parasites that have reached the end of their infection duration are removed from their host's parasite burden.

Design concepts

The model is intended to explore the mathematical consequences of parasite spatial aggregation as simply as

possible to observe patterns clearly. As such, it does not feature any adaptive behavior by individual hosts or parasites. Further, individual hosts do not sense their environment, nor do they interact with one another (e.g., they can share landscape cells). The model's primary aim is to observe parasite burdens among hosts that emerge from the stochastic movement, parasite acquisition, and recovery (or parasite loss) that occur throughout its process. For each host, its burden of parasites is recorded at the end of the simulation (which does not include parasites it has recovered from)—we refer to this as its "snapshot" burden. In addition, the cumulative burden of each host is recorded, that is, the total of all parasites that a host has acquired through the simulation, including those it has recovered from. These burdens can then be summarized at the host population level.

Initialization

At the beginning of a simulation of the model, 96 hosts are randomly distributed about the 48×48 landscape. Each host has zero parasites at timestep 0. The spatial arrangement of landscape cells with parasites varies among different simulations (Figure 1). The density of parasites, or the proportion of cells with parasites, varies from 0.1 to 0.9 in intervals of 0.1. This range covers the parameter space of biological interest—from somewhat rare to extremely common on the landscape, while ignoring scenarios like parasites being absent or occupying every cell. The spatial aggregation of parasites was varied in the model with a "clustering factor" input (used in Figure 1 for demonstration purposes), but it was measured with Moran's *I*. The Moran's *I* values vary from ~0 to 0.2 in inexact intervals as generating a random

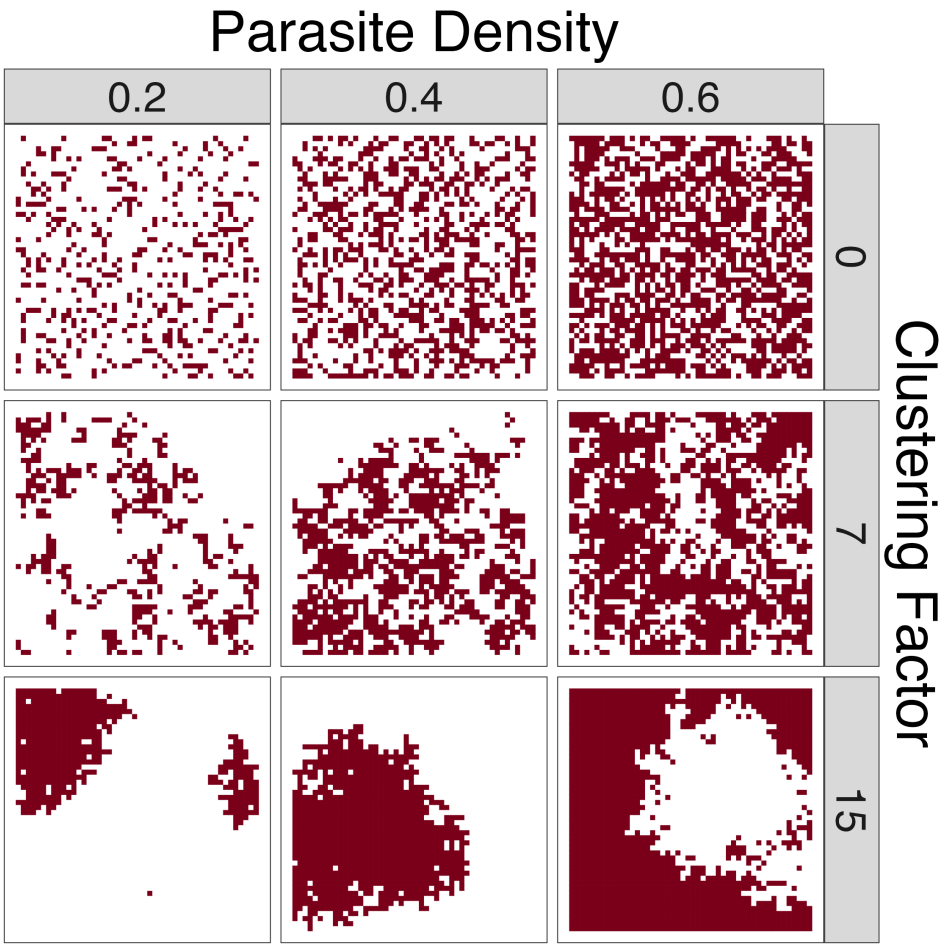

FIGURE 1 Examples of landscape arrangements used in simulations. Dark cells are occupied by parasites. "Parasite Density" refers to the proportion of total cells that are parasite-occupied and increases across panels from left to right. "Clustering Factor" refers to the clustering factor input for the landscape percolation process described in the text and increases from the top row to the bottom row. The clustering factor is highly correlated with Moran's *I* and is used in this figure for consistency of values across rows, as Moran's *I* is too sensitive to specific configuration to easily present landscapes of exactly equal spatial autocorrelation.

landscape with a specific Moran's *I* is not feasible. As Figure 1 shows, this range encompasses random distributions at low "clustering factor"/Moran's *I* and extremely clumped distributions at high "clustering factor"/Moran's *I*, thus representing almost any parasite spatial arrangement that could be observed in nature (except a uniform distribution, which is unlikely for parasites to exhibit). The density and aggregation of parasite-occupied cells both remain constant within a given simulation.

We generated landscape arrangements using a percolation algorithm wherein we start with a blank grid and randomly select one cell to classify as parasite-occupied. Then we successively assign more parasite-occupied cells one by one with the probability of a cell being selected being inversely proportional to its distance to other parasite-occupied cells. In other words, the algorithm assigns parasite-occupied cells based on how close they are to other parasite-occupied cells. The cell assignment repeats until the given proportion of cells (0.1–0.9) has been assigned. The "clustering factor" input modifies the weighting of a cell's probability of being assigned as parasite-occupied. When the clustering factor input is 0, there is no increased probability of selection for cells near previously assigned cells (resulting in a random distribution). As the clustering factor input increases, the probability of selecting a cell based on its proximity to parasite-occupied cells increases.

Input data

Our model does not take any external data as input to inform model processes.

Submodels

Movement

Host movement in each timestep is simulated as a random walk where a host has an equal probability of doing one of the following: remaining in its location, moving one cell up, moving one cell right, moving one cell down, or moving one cell left.

Parasite acquisition

When a host occupies a parasite-occupied cell at the end of a timestep, the number of parasites it gains is a single draw from a binomial distribution with a success probability of 0.5. Thus, a host may gain either one or zero parasites during a timestep (with hosts remaining in the same cell for multiple timesteps having the chance to acquire multiple parasites successively). The probability of parasite acquisition was held constant both within and among simulations, as variation in parasite acquisition is already achieved by the varying parasite densities among simulations.

Parasite recovery/loss

Upon acquisition of a parasite by a host, each parasite is given an infection duration in number of timesteps, which is drawn from a negative binomial distribution with a success probability of either 5%, 15%, or 25% (representing recovery probability or rate). This process is a probabilistic analog to the recovery rate in a traditional compartmental disease model (e.g., a susceptible-infected-recovered model like those discussed in Keeling & Rohani, 2011)—a host has an *X* probability of losing a parasite in a given timestep, and thus on average *X*% of hosts with parasites will lose one in a given time step. These probabilities remain constant within a given simulation but vary among different simulations.

Simulations

We generated 144 total landscapes, each representing a different combination of parasite density and spatial aggregation (Figure 1). Density varied from 0.1 to 0.9 in intervals of 0.1, and clustering factor inputs varied from 0 to 15 in intervals of 1, which corresponded to Moran's *I* values of ~0 to ~0.2. For each recovery probability (5%, 15%, or 25%) and each landscape, we ran 10 separate simulations for 100 timesteps, for a total of 4320 simulations (144 landscape configurations × three recovery rates × 10 replicates).

For each simulation we calculated the dispersion (variance: mean ratio) and Hoover index of the host population's "snapshot" burdens. The dispersion was calculated because it is simple to calculate across a wide variety of scenarios, easy to understand, and can be partially representative of the range of burdens observed. We also calculated the Hoover index, as it is recommended as a measure of aggregation by McVinish and Lester (2020) due to its biological interpretation—it represents the proportion of parasites that would need to be redistributed among hosts so that each host has an equal parasite burden. Accordingly, the index ranges from 0 to 1. Notably, a burden distribution may have a high Hoover index but a low dispersion value if the magnitude of burdens is low throughout all hosts. We also calculated the Pearson correlation coefficients between individual

host "snapshot" and cumulative parasite burdens across host populations at the end of each simulation. We then compared dispersion values, Hoover indices, and correlation coefficients among the different landscapes. A subset of simulations ($n = 360$) was conducted for 1000 timesteps to assess how patterns in dispersion and correlation coefficients change across longer timeframes, showing that 100 timesteps was sufficient for parasite aggregation analyses (Appendix S2). In addition, we ran a larger set of simulations on the same landscape configurations and recovery rates but with 100 replicates each instead of 10. This revealed no qualitative differences in the results of simulations with 10 or 100 replicates per landscape and recovery rate combination (Appendix S3). Here, we show the results from the simulations with 10 replicates to more clearly show individual points in the figures.

RESULTS

Increases in parasite spatial aggregation (Moran's *I*) were associated with increases in host–parasite aggregation as measured by the dispersion of "snapshot" parasite burdens (Figure 2). However, the positive effect of spatial aggregation on parasite burden dispersion was weaker at higher parasite densities. For example, at low Moran's *I* (~0), all parasite density values led to dispersion values less than 2. But at higher Moran's *I* (~0.12–0.18) landscapes with 10% of their cells parasite-occupied resulted in some dispersion values over 6 at the 0.05 recovery rate, while the dispersions of landscapes with 90% of cells parasite-occupied were still less than 2. This effect was dampened with recovery rate, where higher recovery rates led to a reduced increase in dispersion with parasite spatial aggregation, and reduced dispersion values in general. The dispersion values observed from simulations with no parasite spatial aggregation (i.e., the points on the left of each panel) roughly approximate those that might be observed from a non-spatial model; while there are slight differences among spatial and non-spatial implementations, they are not meaningful relative to parasite density or aggregation (see Appendix S1).

Parasite burden Hoover index patterns were generally similar to those of parasite burden dispersion (Figure 3). As parasite spatial aggregation increased, so did the Hoover index. Again, the positive effect of spatial aggregation on dispersion was weaker at higher parasite

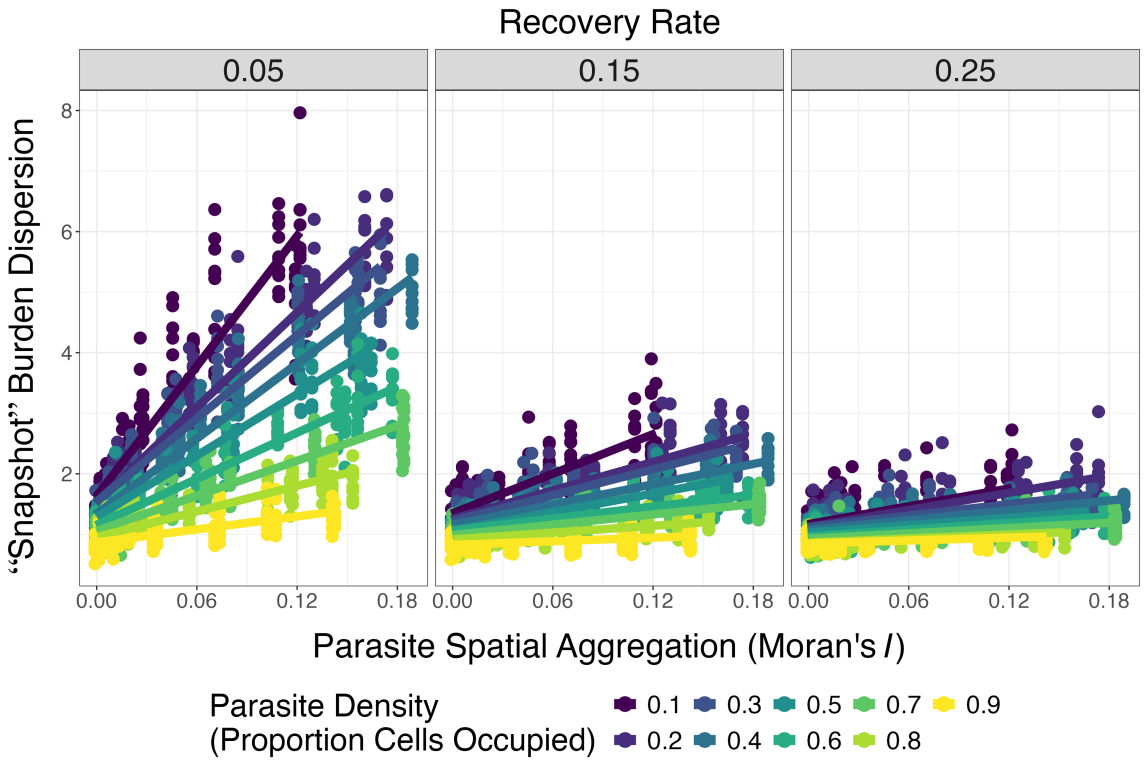

FIGURE 2 The dispersion (variance:mean ratio) of the distribution of "snapshot" parasite burdens of the host population at the end of simulations increases with increasing parasite spatial aggregation, but less so at higher parasite densities. The spatial aggregation of parasites on the landscape, as represented by Moran's *I*, increases along the *X*-axis. Darker colors represent simulations with lower parasite densities, and lighter colors represent higher densities. Each point represents the outcome of one simulation, and the lines represent the average trend for that parasite density level. Each panel displays results from simulations with different recovery rates.

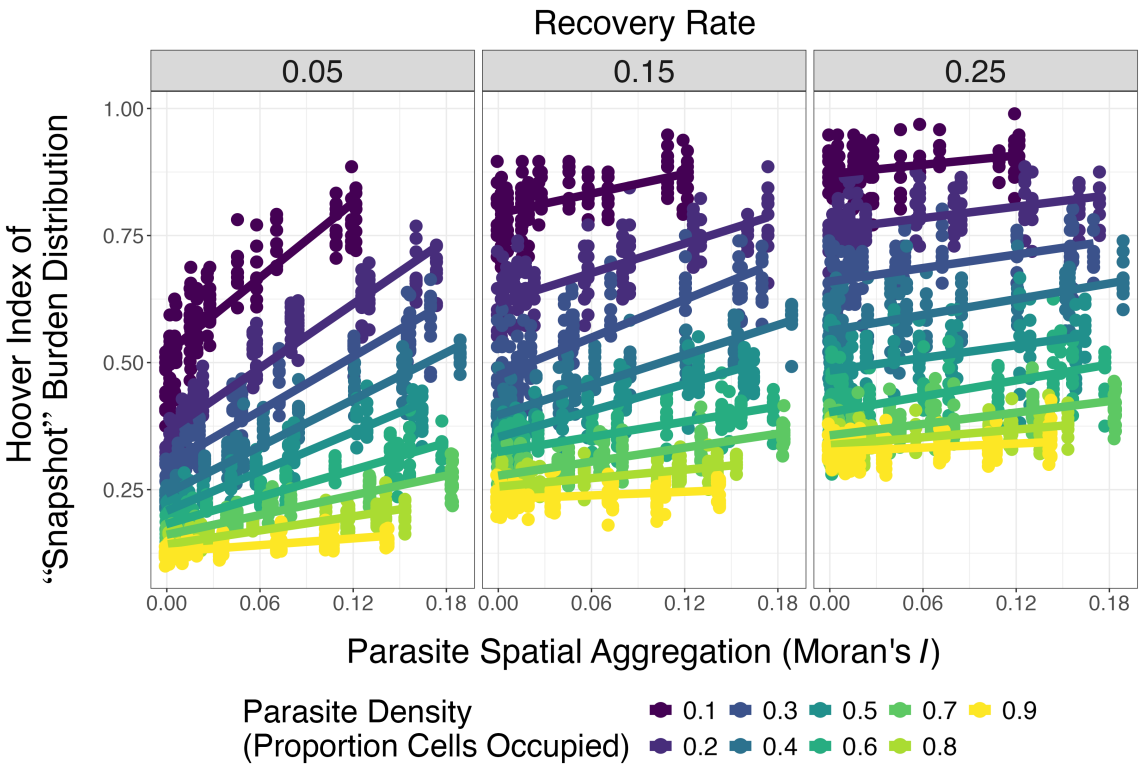

FIGURE 3 The Hoover indices of the distribution of "snapshot" parasite burdens of the host population at the end of simulations increase with increasing parasite spatial aggregation, but less so at higher parasite densities. The spatial aggregation of parasites on the landscape as represented by Moran's *I* increases along the *X*-axis. Darker colors represent simulations with lower parasite densities, and lighter colors represent higher densities. Each point represents the outcome of one simulation, and the lines represent the average trend for that parasite density level. Each panel displays results from simulations with different recovery rates.

density. For example, at the 0.05 recovery rate, landscapes with 10% of their cells occupied by parasites led to Hoover indices around 0.5 at low spatial aggregation (~0 Moran's *I*) but around 0.8 at high spatial aggregation (~0.12 Moran's *I*). Landscapes with 90% parasite-occupied cells, however, led to Hoover indices around 0.15 for all levels of spatial aggregation. In general, as parasite density on the landscape decreased, the Hoover index of "snapshot" burdens increased. At faster recovery rates, Hoover index values remain similar or slightly increase compared to equivalently parameterized simulations at slower recovery rates. This suggests the aggregation of parasite burdens as measured by Hoover's index was observed with a smaller range of values between the least and most parasitized individuals for faster rates of recovery.

In almost every simulation, the correlation between hosts' "snapshot" and cumulative burdens was positive (Figure 4). In other words, hosts with high parasite burdens at the end of a simulation typically also had high parasite burdens throughout the simulation, including parasites that were lost. The strength of the correlation increased with higher parasite spatial aggregation. Slower recovery rates also led to higher correlation coefficients, as it directly reduces the difference between "snapshot" and cumulative burdens (i.e., fewer parasites acquired near the end of the simulation are lost). At a 0.05 recovery rate, correlation coefficients ranged from ~0.5 at low Moran's *I* to ~0.85 at high Moran's *I*, but at a 0.25 recovery rate they only ranged from ~0.25 to ~0.6 at similar Moran's *I* values. Finally, landscapes with higher parasite density had slightly lower correlation coefficients between "snapshot" and cumulative burdens.

DISCUSSION

We assessed how the spatial aggregation of parasites influenced the distribution of parasite burdens among a host population across a range of parasite densities using an agent-based model. Host burdens were highly aggregated when parasite spatial aggregation was high, but less so as the proportion of the landscape occupied by parasites increased. This suggests that the spatial arrangement of environmental or trophically transmitted parasites is most important at low-to-moderate parasite density. Further, spatial aggregation of parasites on the landscape led to high correlation between the parasite burdens of

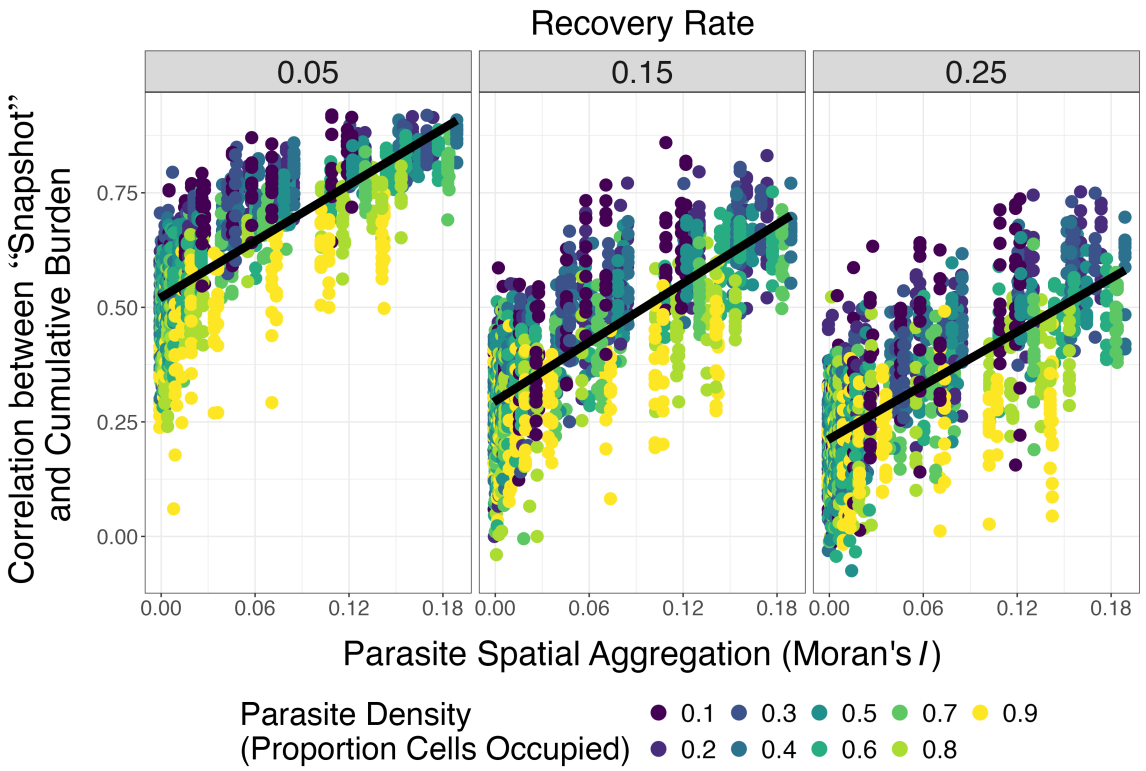

FIGURE 4 The correlation coefficients between individual hosts' "snapshot" parasite burdens (parasite count at simulation end) and cumulative parasite burdens (every parasite acquired, including those lost) increase with parasite clustering. The clustering of parasites on the landscape as represented by Moran's *I* increases along the *X*-axis. Darker colors represent simulations with lower parasite densities, and lighter colors represent higher densities. Each point represents the outcome of one simulation (i.e., the correlation coefficient for the "snapshot" and cumulative burdens of that simulation's population of hosts). The black lines represent the average trend in correlation coefficients with increasing parasite spatial aggregation. Each panel displays results from simulations with different recovery rates.

hosts at simulation end and the parasites they acquired cumulatively throughout the simulation. Thus, observations of hosts with consistently high parasite burdens may be due to spatial aggregation of parasites alone.

The model demonstrates that, all else being equal, spatial aggregation of environmental parasites can lead to the commonly observed pattern of most hosts in a population bearing few, if any, parasites, while a few hosts bear high numbers of parasites. The results of our model match findings from experiments performed on *Tri. confusum* by Keymer and Anderson (1979), where more clustered arrangements of environmental parasites led to greater aggregation of parasite burdens. More specifically, while Keymer and Anderson measured the spatial aggregation of parasites with the variance: mean ratio of parasite eggs in sections of their experimental arena and we used Moran's *I*, we both observed increases in the variance:mean ratio (AKA dispersion) of host–parasite burdens with increases in our respective spatial distribution measures. Spatial variance:mean ratios and Moran's *I* values are not perfect analogs, but they are generally positively correlated, suggesting that our model supports the experimental findings. Further, our work shows that the positive effect of parasite spatial aggregation on host burden dispersion is most likely to be observed when parasite density is low-to-moderate and hosts lose parasites slowly. However, it should be noted that when parasite density is extremely low such that hosts rarely encounter parasites, parasite aggregation on hosts would likely be low irrespective of parasite spatial aggregation. This scenario would represent an "incidental" host of a parasite and, thus, is of less interest in the context of parasite burden aggregation.

Parasite burden aggregation is observed in a diversity of systems, including fish, amphibians, birds, and mammals (Shaw et al., 1998; Shaw & Dobson, 1995), and drivers can be extrinsic (e.g., spatial parasite patterns) or intrinsic to the hosts (e.g., sex or body size). Based on our model, spatial aggregation of parasites has little effect on parasite aggregation on hosts in high parasite density scenarios, which suggests that aggregated host burdens observed in such contexts may be more driven by host characteristics such as sex and/or body size (Devevey & Brisson, 2012), behavior (Boyer et al., 2010), and/or immunity (Johnson & Hoverman, 2014; Tinsley et al., 2020) (which our model did not include). Alternatively,

at low parasite density, the effect of parasite spatial aggregation could overwhelm individual host differences simply by some hosts happening to move through parasite clusters. This relationship between spatial aggregation of parasites and aggregation on hosts is particularly relevant to efforts aiming to understand, model, or control diseases of wildlife or human populations, where parasite aggregation can be of great importance (Rabajante, 2023; Werkman et al., 2020; Wilber et al., 2020).

Our model also suggests that the spatial arrangement of parasites could play a role in the consistency of parasite burdens experienced by hosts over time. If parasite burdens are driven by individual characteristics, it could be assumed that hosts that are observed with high parasite burdens are likely consistently parasitized at those levels due to their attributes. However, our model shows that in the absence of individual differences among hosts, high spatial aggregation of parasites can also lead to consistency in individual parasite burdens over time (Figure 4). In *Peromyscus maniculatus*, specific individuals have been observed to harbor similar tick burdens over successive captures (Devevey & Brisson, 2012), which can be attributed to host characteristics, but our model presents the alternative explanation that while variation among hosts is almost ubiquitous across systems, high spatial aggregation in parasites alone can theoretically lead to consistent burdens on specific hosts. A scenario where parasite burden consistency is wholly explained by parasite spatial distribution is highly unlikely in nature, but the possibility of such a pattern suggests that assumptions of host characteristic-driven burden consistency should be evaluated if the relationship varies widely. Inversely, when parasites are more evenly distributed across the landscape (i.e., spatial aggregation is low) and variation in host attributes is lower, single observations of parasite burdens may be less predictive of lifetime parasite loads. Many studies do not explicitly investigate or report the consistency in individual parasite burdens over time. Thus, future work should consider exploring temporal parasite burden patterns in concert with host attributes and parasite spatial arrangement to further elucidate the drivers of observed parasitism patterns.

Together these results show that in the simple scenario where host organisms are identical, complex patterns of parasitism at the population level can emerge. Simple models can often generate complex behavior; ecological neutral theory has been used to predict patterns of biodiversity based solely on ecological drift (assuming no differences in demographic processes among species in a community), which can be a useful model when compared to empirical systems (Rosindell et al., 2011). Similarly, models like the one presented here that assume no intrinsic differences between individuals within a species may prove to be a useful metric by which to compare empirical parasite burden data (see Gourbière et al., 2015 for another example).

Our model was designed to be tractable and not specific to any given system, thus making its results generalizable for parasite spatial configurations that could be realistically observed across different systems (Levins, 1966). Future work could build upon this model for more specific applications. First, parasites are not exhaustible in the model (i.e., their number is not reduced when acquired by hosts), which is a reasonable simplification in many systems given that free-living parasites or parasites in prey generally vastly outnumber their hosts. However, for scenarios where parasite abundance is limited, the parasite-occupied cells in our model could be made exhaustible. Second, hosts in our model roam nomadically and do not interact with each other. Future models could feature some degree of sociality and/or territoriality in host behavior or incorporate resource selection. For our purposes, using simple movement rules generalizes our results to apply widely and provide baseline predictions before complex movement behavior is considered. Finally, hosts and parasites operate totally independently in the model; that is, hosts do not avoid parasites, nor is their behavior influenced by the number they have acquired. Again, this generalizes our results, given that different systems may feature parasite avoidance or the opposite when parasites are associated with resources, and movement behavior can change in different ways with infection depending on the organism. Finally, parasites lost by hosts disappear from the model, which is a reasonable simplification for multi-host environmental parasites or parasites that are gained via consumption, but not so for single-host environmental parasites (though spatial heterogeneity may manifest differently in such cases). Future work could implement one or more of these complexities to extend the model and provide more insight into how the role of space in parasite aggregation changes among different contexts. In addition, our results could be tested empirically with a large-scale, manipulative field experiment, wherein parasites are placed in the environment with different densities and spatial arrangements across treatments.

This model provides explicit mathematical evidence of the potential for spatial aggregation of environmental or trophically transmitted parasites to drive varying patterns of parasite burdens in host populations. The uncomplicated implementation provides a resultingly straightforward interpretation that points toward contexts of low-moderate parasite density combined with suspected spatial aggregation of parasites as being scenarios where spatial arrangement may be most important.

Future theoretical work could explore how robust these results are to modifying parasite ecology or host behavior, and empirical studies could more explicitly investigate the consistency of parasite burdens with reference to their spatial arrangement. Overall, this work serves as a theoretical indication that fine-scale spatial patterns of parasites can be highly influential in certain contexts.

AUTHOR CONTRIBUTIONS

Chris Wojan developed the idea, wrote the simulation code, and was the primary writer of the manuscript, while Allison K. Shaw and Meggan E. Craft provided crucial guidance in framing and conducting theoretical research, as well as assisted in manuscript drafting and revising.

ACKNOWLEDGMENTS

We would like to thank John Fieberg, Susan Jones, Dennis Kim, Katie Krueger, Jack Lawson, Clarence Lehman, Lisa Meyer, Matt Michalska-Smith, Janine Mistrick, David Munkvold, Naven Narayanan, Eric Seabloom, Molly Simonis, Martha Torstenson, Meredith VanAcker, Lauren White, Mingzi Xu, Marlene Zuk, and anonymous reviewers for their valuable feedback and advice at various stages of the work.

CONFLICT OF INTEREST STATEMENT

The authors declare no conflicts of interest.

DATA AVAILABILITY STATEMENT

Data and code (Wojan, 2025) are available from Zenodo: https://doi.org/10.5281/zenodo.15360216.

ORCID

Chris Wojan https://orcid.org/0000-0003-1783-9163
Allison K. Shaw https://orcid.org/0000-0001-7969-8365

REFERENCES

Albery, G. F., D. J. Becker, F. Kenyon, D. H. Nussey, and J. M. Pemberton. 2019. "The Fine-Scale Landscape of Immunity and Parasitism in a Wild Ungulate Population." *Integrative and Comparative Biology* 59: 1165–75. https://doi.org/10.1093/icb/icz016.

Albery, G. F., A. R. Sweeny, D. J. Becker, and S. Bansal. 2022. "Fine-Scale Spatial Patterns of Wildlife Disease Are Common and Understudied." *Functional Ecology* 36: 214–225. https://doi.org/10.1111/1365-2435.13942.

Bengtsson, H. 2021. "A Unifying Framework for Parallel and Distributed Processing in R Using Futures." *The R Journal* 13: 208. https://doi.org/10.32614/RJ-2021-048.

Bonnell, T. R., R. R. Ghai, T. L. Goldberg, R. Sengupta, and C. A. Chapman. 2018. "Spatial Configuration Becomes more Important with Increasing Habitat Loss: A Simulation Study of Environmentally-Transmitted Parasites." *Landscape Ecology* 33: 1259–72. https://doi.org/10.1007/s10980-018-0666-4.

Boyer, N., D. Réale, J. Marmet, B. Pisanu, and J.-L. Chapuis. 2010. "Personality, Space Use and Tick Load in an Introduced Population of Siberian Chipmunks *Tamias sibiricus*." *Journal of Animal Ecology* 79: 538–547. https://doi.org/10.1111/j.1365-2656.2010.01659.x.

Calabrese, J. M., J. L. Brunner, and R. S. Ostfeld. 2011. "Partitioning the Aggregation of Parasites on Hosts into Intrinsic and Extrinsic Components Via an Extended Poisson-Gamma Mixture Model." *PLoS One* 6: e29215. https://doi.org/10.1371/journal.pone.0029215.

Devevey, G., and D. Brisson. 2012. "The Effect of Spatial Heterogenity on the Aggregation of Ticks on White-Footed Mice." *Parasitology* 139: 915–925. https://doi.org/10.1017/S003118201200008X.

Dominik, A. 2024. "som.nn: Topological k-NN Classifier Based on Self-Organising Maps." R package version 1.4.4. https://CRAN.R-project.org/package=som.nn.

Dumas, A., C. Bouchard, L. R. Lindsay, N. H. Ogden, and P. A. Leighton. 2022. "Fine-Scale Determinants of the Spatiotemporal Distribution of *Ixodes scapularis* in Quebec (Canada)." *Ticks and Tick-borne Diseases* 13: 101833. https://doi.org/10.1016/j.ttbdis.2021.101833.

Ginsberg, H. S., E. L. Rulison, J. L. Miller, G. Pang, I. M. Arsnoe, G. J. Hickling, N. H. Ogden, R. A. LeBrun, and J. I. Tsao. 2020. "Local Abundance of *Ixodes scapularis* in Forests: Effects of Environmental Moisture, Vegetation Characteristics, and Host Abundance." *Ticks and Tick-borne Diseases* 11: 101271. https://doi.org/10.1016/j.ttbdis.2019.101271.

Gourbière, S., S. Morand, and D. Waxman. 2015. "Fundamental Factors Determining the Nature of Parasite Aggregation in Hosts." *PLoS One* 10: e0116893. https://doi.org/10.1371/journal.pone.0116893.

Grimm, V., U. Berger, F. Bastiansen, S. Eliassen, V. Ginot, J. Giske, J. Goss-Custard, et al. 2006. "A Standard Protocol for Describing Individual-Based and Agent-Based Models." *Ecological Modelling* 198: 115–126. https://doi.org/10.1016/j.ecolmodel.2006.04.023.

Grimm, V., U. Berger, D. L. DeAngelis, J. G. Polhill, J. Giske, and S. F. Railsback. 2010. "The ODD Protocol: A Review and First Update." *Ecological Modelling* 221: 2760–68. https://doi.org/10.1016/j.ecolmodel.2010.08.019.

Grimm, V., S. F. Railsback, C. E. Vincenot, U. Berger, C. Gallagher, D. L. DeAngelis, B. Edmonds, et al. 2020. "The ODD Protocol for Describing Agent-Based and Other Simulation Models: A Second Update to Improve Clarity, Replication, and Structural Realism." *Journal of Artificial Societies and Social Simulation* 23(7): 7. https://doi.org/10.18564/jasss.4259.

Harrison, A., and N. C. Bennett. 2012. "The Importance of the Aggregation of Ticks on Small Mammal Hosts for the Establishment and Persistence of Tick-Borne Pathogens: An Investigation Using the R 0 Model." *Parasitology* 139: 1605–13. https://doi.org/10.1017/S0031182012000893.

Johnson, P. T. J., and J. T. Hoverman. 2014. "Heterogeneous Hosts: How Variation in Host Size, Behaviour and Immunity Affects Parasite Aggregation." *Journal of Animal Ecology* 83: 1103–12. https://doi.org/10.1111/1365-2656.12215.

Keeling, M. J., and P. Rohani. 2011. *Modeling Infectious Diseases in Humans and Animals*. Princeton, NJ: Princeton University Press.

Keymer, A. E., and R. M. Anderson. 1979. "The Dynamics of Infection of *Tribolium confusum* by *Hymenolepis diminuta*: The Influence of Infective-Stage Density and Spatial Distribution." *Parasitology* 79: 195–207. https://doi.org/10.1017/S0031182000053282.

Levins, R. 1966. "The Strategy of Model Building in Population Biology." *American Scientist* 54: 421–431.

Lutermann, H., K. Medger, and I. G. Horak. 2012. "Abiotic and Biotic Determinants of Tick Burdens in the Eastern Rock Sengi (*Elephantulus myurus*)." *Medical and Veterinary Entomology* 26: 255–262. https://doi.org/10.1111/j.1365-2915.2011.01002.x.

Mathieu-Bégné, E., S. Blanchet, O. Rey, O. Scelsi, C. Poesy, G. Marselli, and G. Loot. 2022. "A Fine-Scale Analysis Reveals Microgeographic Hotspots Maximizing Infection Rate between a Parasite and its Fish Host." *Functional Ecology* 36: 380–391. https://doi.org/10.1111/1365-2435.13967.

Mathisson, D. C., S. M. Kross, M. I. Palmer, and M. A. Diuk-Wasser. 2021. "Effect of Vegetation on the Abundance of Tick Vectors in the Northeastern United States: A Review of the Literature." *Journal of Medical Entomology* 58: 2030–37. https://doi.org/10.1093/jme/tjab098.

McVinish, R., and R. J. G. Lester. 2020. "Measuring Aggregation in Parasite Populations." *Journal of the Royal Society Interface* 17: 20190886. https://doi.org/10.1098/rsif.2019.0886.

Mollison, D., and S. A. Levin. 1995. "Spatial Dynamics of Parasitism." In *Ecology of Infectious Diseases in Natural Populations*, First ed., edited by B. T. Grenfell and A. P. Dobson, 384–398. Cambridge: Cambridge University Press.

Nunn, C. L., P. H. Thrall, F. H. Leendertz, and C. Boesch. 2011. "The Spread of Fecally Transmitted Parasites in Socially-Structured Populations." *PLoS One* 6: e21677. https://doi.org/10.1371/journal.pone.0021677.

Paradis, E., and K. Schliep. 2019. "ape 5.0: An Environment for Modern Phylogenetics and Evolutionary Analyses in R." *Bioinformatics* 35: 526–28. https://doi.org/10.1093/bioinformatics/bty633.

R Core Team. 2024. *R: A Language and Environment for Statistical Computing*. Vienna: R Foundation for Statistical Computing.

Rabajante, J. F. 2023. "On Spatiotemporal Overdispersion and Macroparasite Accumulation in Hosts Leading to Aggregation: A Quantitative Framework." *Diseases* 11: 4. https://doi.org/10.3390/diseases11010004.

Rosindell, J., S. P. Hubbell, and R. S. Etienne. 2011. "The Unified Neutral Theory of Biodiversity and Biogeography at Age Ten." *Trends in Ecology & Evolution* 26: 340–48. https://doi.org/10.1016/j.tree.2011.03.024.

Shaw, D. J., and A. P. Dobson. 1995. "Patterns of Macroparasite Abundance and Aggregation in Wildlife Populations: A Quantitative Review." *Parasitology* 111: S111–S133. https://doi.org/10.1017/S0031182000075855.

Shaw, D. J., B. T. Grenfell, and A. P. Dobson. 1998. "Patterns of Macroparasite Aggregation in Wildlife Host Populations." *Parasitology* 117: 597–610. https://doi.org/10.1017/S0031182098003448.

Tinsley, R. C., H. R. Vineer, R. Grainger-Wood, and E. R. Morgan. 2020. "Heterogeneity in Helminth Infections: Factors Influencing Aggregation in a Simple Host–Parasite System." *Parasitology* 147: 65–77. https://doi.org/10.1017/S003118201900129X.

Vaughan, D., and M. Dancho. 2022. "furrr: Applying Mapping Function in Parallel using Futures." R package version 0.3.1. https://CRAN.R-project.org/package=furrr.

Werkman, M., J. E. Wright, J. E. Truscott, W. E. Oswald, K. E. Halliday, M. Papaiakovou, S. H. Farrell, R. L. Pullan, and R. M. Anderson. 2020. "The Impact of Community-Wide, Mass Drug Administration on Aggregation of Soil-Transmitted Helminth Infection in Human Host Populations." *Parasites & Vectors* 13: 1–12. https://doi.org/10.1186/s13071-020-04149-4.

Wickham, H., M. Averick, J. Bryan, W. Chang, L. McGowan, R. François, G. Grolemund, et al. 2019. "Welcome to the Tidyverse." *Journal of Open Source Software* 4: 1686. https://doi.org/10.21105/joss.01686.

Wilber, M. Q., C. J. Briggs, and P. T. J. Johnson. 2020. "Disease's Hidden Death Toll: Using Parasite Aggregation Patterns to Quantify Landscape-Level Host Mortality in a Wildlife System." *Journal of Animal Ecology* 89: 2876–87. https://doi.org/10.1111/1365-2656.13343.

Wilson, K., O. N. Bjørnstad, A. P. Dobson, S. Merler, G. Poglayen, S. E. Randolph, A. F. Read, and A. Skorping. 2002. "Heterogeneities in Macroparasite Infections: Patterns and Processes." In *The Ecology of Wildlife Diseases*, edited by P. J. Hudson, A. Rizzoli, B. T. Grenfell, H. Heesterbeek, and A. P. Dobson, 6–44. Oxford: Oxford University Press.

Wojan, C. 2025. "cwojan/spatially_aggregated_parasite: spatially_aggregated_parasite." Zenodo. https://doi.org/10.5281/zenodo.15360216.

SUPPORTING INFORMATION

Additional supporting information can be found online in the Supporting Information section at the end of this article.

How to cite this article: Wojan, Chris, Allison K. Shaw, and Meggan E. Craft. 2025. "Parasite Spatial Distribution Shapes Parasite Aggregation on Host Populations, but Not at High Parasite Density." *Ecosphere* 16(6): e70324. https://doi.org/10.1002/ecs2.70324